SIGNATURE OF CURRENT SHEETS AS SEEN BY TIP AT VTT IN THE HeI MULTIPLET AT 1083.0 nm

R. Aznar Cuadrado[1], S. K. Solanki[1], A. Lagg[1], R. M. Thomas[1]

[1] *Max-Planck-Institut für Sonnensystemforschung, Max-Planck-Str. 2, 37191 Katlenburg-Lindau, Germany, Email:aznar,solanki,lagg,thomasr@mps.mpg.de*

ABSTRACT

We report infrared spectropolarimetric observations obtained with the Tenerife Infrared Polarimeter (TIP) at the German Vacuum Tower Telescope (VTT) of the Spanish observatory of Izaña, Tenerife. The observations taken in the chromospheric He I 1083.0 nm multiplet were used to create maps in the Stokes parameters *I*, *Q*, *U* and *V*. A number of active regions have been scanned. A technique to invert Stokes profiles of the He I 1083.0 nm multiplet lines was applied in order to obtain the full magnetic vector and the line-of-sight velocity. Here initial results are presented. Evidence for electric current sheets separating regions of opposite polarities has been found in at least 3 active regions. Rapid flows with line-of-sight velocities of the order of 30-50 km s^{-1} turn out to quite common and are generally found in several locations of most observed active regions.

1. OBSERVATIONS AND INSTRUMENTATION

Observations of several active regions were carried out with the Tenerife Infrared Polarimeter (TIP) at the Vacuum Tower Telescope (VTT), Izaña Observatory, Tenerife, during May 2001 and August 2003. The spectrograph spectral resolution was 30 mÅ per pixel and the pixel size was 0.4". The observed wavelength range, from 1082.5 to 1083.3 nm, contains two photospheric lines of Si I (at 1082.709 nm, effective Landé factor g_{eff} = 1.5) and Ca I (at 1082.93 nm), the chromospheric He I multiplet (He Ia at 1082.909 nm, He Ib at 1083.025 nm and He Ic at 1083.034 nm, with g_{eff} = 2.0, 1.75 and 1.25, respectively) and a telluric blend at 1083.21 nm. A typical exposure time of 5 seconds per slit position was used in all scanned regions presented in this work. Flat-field, calibration and dark current measurements were obtained before and after each scan to correct the measurements.

Table 1 reports some details of the observations presented in this work. The angle $\mu = \cos\theta$, where θ is the heliocentric angle, i.e. the angle between the line-of-sight and the normal to the solar surface. UT is the universal time at the beginning of each observation. In order to increase the signal-to-noise level, all spectra were binned over three spectral pixels.

Table 1. Observational details

Date	NOAA	Solar Position	θ (deg)	μ	UT	S/N
13/05/2001	9451	33°W 23°S	41	0.80	15:06	245
22/08/2003	10441	36°E 10°N	40	0.81	18:04	485
26/08/2003	10441	11°W 13°N	13	0.98	09:09	507
26/08/2003	10445	35°E 4°N	40	0.81	08:00	485
27/08/2003	10436	56°W 11°N	61	0.57	09:54	330

1.1 Wavelet Based Denoising

The wavelet representation of a signal offers greater flexibility in de-noising astronomical spectra as compared to classical Fourier smoothing, due to the additional wavelength resolution of the decomposed signal. The method used for de-noising our data is similar to a wavelet packet analysis using non-orthogonal wavelets. The highest frequency coefficients are generally dominated by noise but a considerable amount of signal could be hidden in them. Therefore, truncating them blindly would lead to a loss of information. This is resolved by using a wavelet packet approach wherein the signal at each of the frequency scales is treated as a new noisy signal and then is further decomposed. The signal, afterwards, is truncated using a suitable threshold.

The high redundancy of the non-orthogonal base we use in our version of the wavelet transform, namely the *a'trous* algorithm (Holschneider & Tchamitchian, 1990), allows the main features of the uncorrupted signal to be recovered even after several decompositions. The program is implemented such that the number of scales, which are the frequency partitions and levels of decomposition (i.e., the number of times you want to split the signal at a particular frequency) can be chosen and optimized for a class of signals. See Fligge & Solanki (1997) for an illustrated example of such an application.

2. CURRENT SHEET CRITERIA

Electric current sheets are sharp boundaries separating regions of opposite magnetic polarity. Hence, a minimum of the magnetic field should be present at that boundary. A large jump of the magnetic field inclination angle between the two regions (ideally close to 180°) is also necessary. The azimuthal direction of the magnetic field vector is normally parallel to the current sheet. The first two requirements for a current sheet to be present can be detected by means of the analysis of the Stokes *V* profile, while the azimuthal angle of the magnetic field is only measurable through the inversion of the full magnetic vector (i.e. Stokes *Q* and *U* are also necessary).

3. STOKES *V* ANALYSIS

Regions with opposite polarities were identified by studying the sign and strength of the Stokes *V* vector of the He I doublet at 1083.0 nm. Fig. 1 shows maps of active regions where the peak of the *V*-signal of the HeI doublet lies at different $\sigma(V)$ levels. The $\sigma(V)$ level is obtained from the standard deviation value of Stokes *V* profiles over a continuum window of 20 pixels (see Table 2). In Fig. 1 white and black colour represent maximum and minimum values, respectively, of the colour scale. Pores present in the continuum intensity maps are represented by green isocontours.

A first requirement on a (vertically oriented) electric current sheet is that it sharply separates two areas of opposite magnetic polarity. All active regions shown in Fig. 1 present quite sharp boundaries of opposite polarities, which is an indication of possible current sheets. Light-blue ellipses identify positions where a current sheet may be present. However, further tests are needed to confirm this (see Sect. 4).

4. INVERSION OF THE FULL MAGNETIC VECTOR

The He I triplet (nearly optically thin, but with a complex non-LTE formation) was analysed by inverting the data using the Unno-Rachkowsky solution to describe the individual Zeeman components of each

Table 2. Maximum speeds of the HeI upflow and downflow components and σ (*V*) level of each scan.

Date	NOAA	Max. v_{upflow} (km s^{-1})	Max. $v_{downflow}$ (km s^{-1})	σ (*V*) (x10^{-4})
13/05/2001	9451	- 5	33	3.80
22/08/2003	10441	-18	30	5.29
26/08/2003	10441	- 5	35	6.11
26/08/2003	10445	-12	44	6.58
27/08/2003	10436	-14	57	7.88

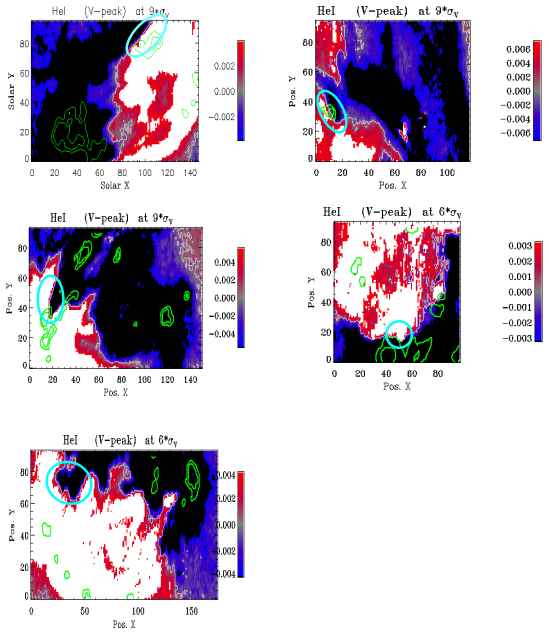

Figure 1. Maps of magnetic polarity for pixels with V-peaks at different σ(V) levels of active regions: NOAA 9451 (top-left panel); NOAA 10436 (top-right); NOAA 10441 (middle-left, on 26/08/03), NOAA 10441(middle-right, on 22/08/03) and NOAA 10445 (bottom-left). Sign of *V-polarity: red is right-handed, blue is left-handed.*

member of the triplet (method described in Lagg *et al.* 2003). The inversion allows us to retrieve the full magnetic vector in the upper chromosphere (where the He I triplet is formed), including the strength of the magnetic field, its inclination to the solar surface normal and its direction in the horizontal plane (i.e., the azimuthal angle). Since the He Ia line is blended by a photospheric Ca I line, the analysis is essentially based on the He Ib and He Ic lines, which are free of blends. Line-of-sight velocity maps are also obtained (positive values of velocity denote downflows).

4.1 Current Sheet

The maps of some parameters derived from the inversion of the two strongest He I lines are displayed in the left panel of Fig. 2. The top-left panel shows the magnetic field strength, revealing locations of strong gradients in the magnetic vector. The right panel of Fig. 2 clearly shows the abrupt drop of the field strength along a neutral line, forming a deep valley whose width corresponds closely to the estimated spatial resolution of 1.5" characterising these observations. This magnetic field configuration will lead to an electric current flowing parallel to the solar surface along the direction of the discontinuity in the field direction. Using Ampère's law we can estimate the lower limit of the current density to be 90 mA/m^2.

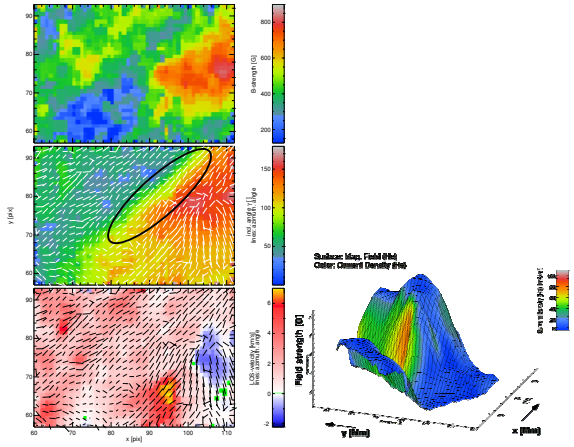

Figure 2. Left panel: atmospheric parameters of the emergent flux active region NOAA 9451 obtained in the strongest He Ib and He Ic lines around the position of a current sheet (black solid ellipse). Right panel: representation of the electric current sheet.

Middle- and bottom-left panels show the inclination angle and the line-of-sight velocity, respectively, with overplotted the azimuthal angle (white and black dashes). The azimuthal direction of the magnetic field vector is parallel to the current sheet, implying that the current sheet is indeed a separatrix between two distinct magnetic regions (see Solanki *et al.* 2003).
Several C-class flares were reported in NOAA 9451 during the day of the observation, so that this strong current sheet may have triggered off such events.

4.2 Possible Current Sheets

Fig. 3 show the atmospheric parameters returned by a 1-component inversion of a region close to a possible current sheet of active regions NOAA 10445 (left panel) and NOAA 10441 (observed on 22/08/03, right panel). In both regions a change of inclination angle is present over a large number of pixels at the positions where the Stokes *V* analysis shows a sharp boundary of opposite polarities (see Fig. 1: NOAA 10445 in bottom-left panel; NOAA 10441 in middle-right panel) and where the azimuthal direction is parallel to the possible current sheet (indicated by black solid ellipses).

4.3 No Current Sheets

The two active regions presented in Fig. 4, NOAA 10441 (observed on 26/08/03, left panel) and NOAA 10436 (right panel), do not fulfill the requirement of the azimuthal angle being parallel to the current sheet, although the Stokes *V* analysis (see Fig. 1: NOAA 10436 in top-right panel; NOAA 10441 in middle-left panel) showed a sharp boundary between opposite polarities.

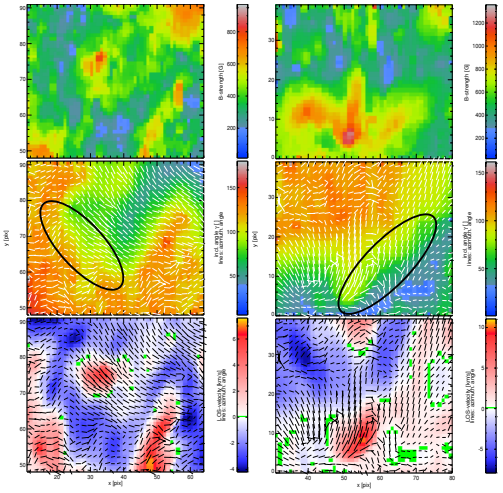

Figure 3. Atmospheric parameters returned by a 1-component inversion of a region around possible current sheets in active regions: NOAA 10445 (left panel) and NOAA 10441(observed on 22/08/03, right panel).

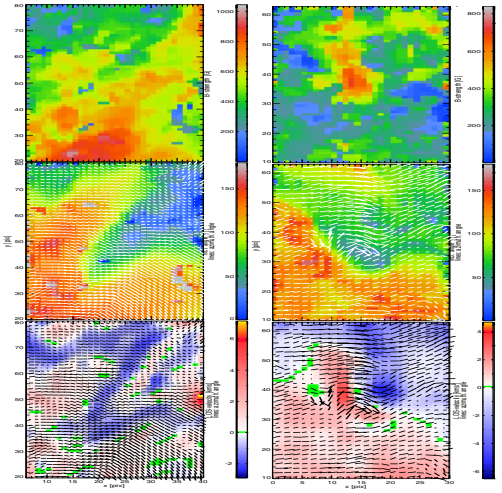

Figure 4. As in Fig. 3 for active regions: NOAA 10441 (observed on 26/08/03, left panel) and NOAA 10436 (right panel).

5. THREE-COMPONENT ATMOSPHERE

Fig. 5 presents a typical profile of one He I component at rest obtained in active region NOAA 10436. The magnetic and velocity parameters returned for this location are: B = 450 G and v = 2 km s^{-1}. The chromospheric maps show a region with strong downflow velocities, where the 1-component analysis is

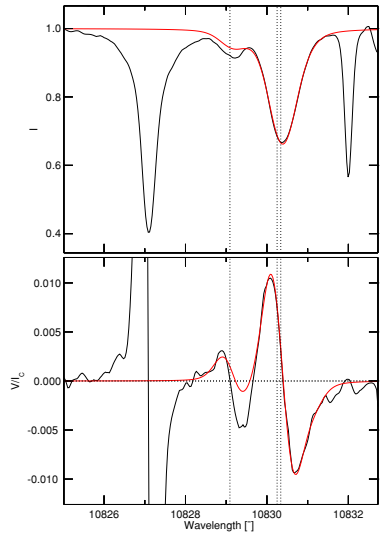

Figure 5. 1-component fit obtained at a given pixel of NOAA 10436 to the He I doublet at 1083.0 nm. Black solid line is the observed profile while red solid line is the fitted profile. The three vertical dotted lines show the rest position of the chromospheric He I multiplet.

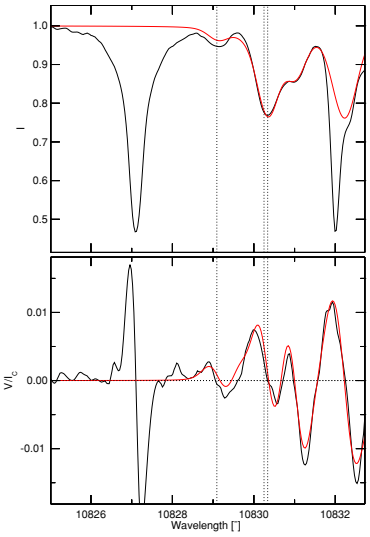

Figure 6. Profile showing three magnetic components obtained in NOAA 10436.

not optimal. At such locations two component fits often provide a much better representation of the flows. However, we have found cases where even a third component is necessary.

An example of a spectrum, recorded in NOAA 10436, that requires a 3-component analysis of Stokes *I* and V/I_c is shown in Fig. 6 (black curves). Such an analysis (red curves, representing the synthetic spectrum) clearly identifies a slow component (1 km s^{-1}) and two fast components (20 and 53 km s^{-1}, respectively). The magnetic field strength of the three components are: 330, 800 and 360 Gauss, respectively. Note that the photospheric Si I line at 1082.71 nm shows only a single component.

Table 2 reports the maximum values of upflow and downflow velocities measured in the He I doublet at 1083.0 nm for the datasets presented in this work. In all cases a second He I component was necessary to fit the four Stokes vectors (with light-of-sight velocities of the order of 30-40 km s^{-1}), and in one case (NOAA 10436) also a third component was needed to fit the observed profiles, as seen in Fig. 6.

6. CONCLUSIONS

We have shown that the inversion of the full magnetic vector is important in order to detect current sheets. From a total of roughly 12 scanned active regions, only 3 showed strong evidence for a current sheet, indicating that detectable current sheets are not very common. The optimal configuration for this detection is when the current sheet is pointing towards the observer. Hence, the detection of current sheets is limited by geometric effects, i.e., current sheets are more likely to be detectable when the line-of-sight is in the direction of the plane of the current sheet. This could mean that current sheets may be more common than our analysis suggests.

7. REFERENCES

Fligge M. and Solanki S. K., *A&AS,* Vol. 124, 579-587, 1997.

Holschneider M. and Tchamitchian P., *Les ondelettes*, ed. P.G. Lemaire (Springer-Verlag), 1990.

Lagg A., Woch J., Krupp N. and Solanki S. K., *A&A*, Vol. 414, 1109-1120, 2004.

Solanki S. K., Lagg A., Woch N., Krupp N. and Collados M., *Nature,* Vol. 425, 692-695, 2003.